Furthermore, it was noted that the visible absorption maxima of oxalato complexes were very close to each other (Table III). The isopropyl groups of 3,9-Ip_2-2,3,2-tet brought about no remarkable decrease of the ligand field strength of the tetraamine in comparison with others. It was presumed, therefore, that the steric effects caused by the isopropyl group attached to the carbon adjacent to the secondary nitrogen are not so significant as to exclude the formation of *trans*-dichloro complex with 3,9-Ip_2-2,3,2-tet. Molecular model examines also suggests no obvious stereochemical reason for the fact that *trans*-(*RR*)-$[CoCl_2(3,9\text{-}Ip_2\text{-}2,3,2\text{-tet})]^+$ is not produced even from the carbonato complex.

As described previously,[10,11] the isomerization from Λ-*cis*-β-(*RR*)- to *trans*-(*RR*)-$[CoCl_2(2,10\text{-}Me_2\text{-}2,3,2\text{-tet})]^+$ proceeds without difficulty in hydrochloric acid solution and is usually facilitated by the addition of perchlorate ion, which enhances particularly the crystallization of *trans*-dichlorocobalt(III) complex. Similar enhanced crystallization of *trans*-(*RR*)-dichloro complexes could be observed for 3,9-Me_2-, 2,10-Ip_2-, and 2,10-Bn_2-2,3,2-tet in this study. A plausible explanation for the exceptional case of 3,9-Ip_2-2,3,2-tet may be that Λ-*cis*-β(*RR*)-$[CoCl_2(3,9\text{-}Ip_2\text{-}2,3,2\text{-tet})]^+$, which can be developed from Λ-β-(*RR*)-$[CoCO_3(3,9\text{-}Ip_2\text{-}2,3,2\text{-tet})]^+$, isomerizes to the corresponding *trans*-(*RR*)-dichloro complex only very slowly and/or the trans complex is highly soluble even as the perchlorate salt.

Acknowledgment. This work was supported by a Grant-in-Aid for Scientific Research from the Ministry of Education, Science and Culture (Grant No. 56209002).

Registry No. *trans*-(*RR*)-$[CoCl_2(2,10\text{-}Ip_2\text{-}2,3,2\text{-tet})]ClO_4$, 94404-88-3; *trans*-(*RR*)-$[CoCl_2(2,10\text{-}Bn_2\text{-}2,3,2\text{-tet})]ClO_4$, 94404-90-7; *trans*-(*RS*)-$[CoCl_2(2,10\text{-}Bn_2\text{-}2,3,2\text{-tet})]ClO_4$, 94481-28-4; *trans*-(*RR*)-$[CoCl_2(2,10\text{-}Me_2\text{-}2,3,2\text{-tet})]ClO_4$, 60801-69-6; *trans*-(*RR*)-$[CoCl_2(2,3,2\text{-tet})]^+$, 27957-84-2; *trans*-(*RS*)-$[CoCl_2(3,9\text{-}Me_2\text{-}2,3,2\text{-tet})]^+$, 73396-01-7; *trans*-(*RS*)-$[CoCl_2(2,10\text{-}Ip_2\text{-}2,3,2\text{-tet})]^+$, 94481-29-5; Λ-β-$[CoCO_3(2,10\text{-}Bn_2\text{-}2,3,2\text{-tet})]ClO_4$, 94404-92-9; Λ-β-$[Co(C_2O_4)(3,9\text{-}Ip_2\text{-}2,3,2\text{-tet})]ClO_4$, 94404-94-1; Λ-β-$[Co(C_2O_4)(2,10\text{-}Ip_2\text{-}2,3,2\text{-tet})]Cl$, 94426-36-5; Λ-β-$[Co(C_2O_4)(2,10\text{-}Bn_2\text{-}2,3,2\text{-tet})]ClO_4$, 94404-96-3; Λ-β-$[Co(C_2O_4)(3,9\text{-}Me_2\text{-}2,3,2\text{-tet})]ClO_4$, 94404-98-5; *trans*-$[CoCl_2(3,9\text{-}Me_2\text{-}2,3,2\text{-tet})]ClO_4$, 73396-02-8; Λ-β-$[Co(C_2O_4)(2,10\text{-}Me_2\text{-}2,3,2\text{-tet})]ClO_4$, 94405-00-2; $Na_3[Co(CO_3)_3]$, 75632-02-9; $K_3[Co(C_2O_4)_3]$, 14239-07-7; 2,10-Bn_2-2,3,2-tet, 94405-01-3; 2,10-Ip_2-2,3,2-tet, 94405-03-5; 3,9-Ip_2-2,3,2-tet, 94405-04-6; *N*-(*tert*-butyloxy)carbonyl-L-phenylalanine, 13734-34-4; 1,3-propanediamine, 109-76-2; *N*,*N'*-bis(*N*-*tert*-butyloxy)carbonyl-L-phenylalanyl)-1,3-propanediamine, 94405-02-4; (*tert*-butyloxy)carbonyl-L-valine, 13734-41-3; L-valinol, 2026-48-4; 1,3-dichloropropane, 142-28-9.

Contribution from the CNRS, UA 403, Ecole Nationale
Supérieure de Chimie, 75231 Paris Cédex 05, France

Chiral Octahedral Iron and Ruthenium Complexes. Use of Diastereotopic Phosphorus Atoms for the Direct Observation of Hidden Coupling Constants

MAREK PAŇKOWSKI,* WLADYSLAW CHODKIEWICZ, and MARIE-PAULE SIMONNIN

Received May 25, 1984

A series of asymmetric phosphorus ligands was synthesized and used to prepare chiral octahedral iron and ruthenium complexes $(MR(CO)_2L^*(PMe_3)_2)^+A^-$. Their geometrical configuration was deduced from IR and NMR (^1H, ^{31}P) spectroscopic studies. Due to the presence of an asymmetric center directly bonded to the metal atom, the two axial PMe_3 ligands are shown to be diastereotopic and this allows, for the first time, a direct determination of the phosphorus–phosphorus coupling constants between chemically identical ligands by ^{31}P NMR. The conformation of the asymmetric ligands relative to the other ligands, CO, R, and the two axial PMe_3 groups, is shown to be an important factor in determining the magnitude of the proton inequivalence between the two PMe_3 ligands.

Introduction

Octahedral complexes having two identical ligands L in mutually trans positions possess a symmetry plane. This equatorial plane is the sole element of symmetry if the four equatorial ligands are different, $a \neq b \neq c \neq d$, or if two of these ligands are identical but have a cis orientation, $a = b \neq c \neq d$ (C_s symmetry).

Removal of the symmetry plane can be achieved by introducing an asymmetric ligand in the equatorial plane. Although the metal itself is not an asymmetric center, such complexes having no symmetry element are chiral and belong to the C_1 symmetry group. Therefore the axial ligands L are diastereotopic.

This report describes the synthesis of iron and ruthenium chiral octahedral complexes **1**, where the equatorial ligand L* is asymmetric. A number of two-electron ligands were used, but special attention was focused on asymmetric phosphines where an atom of phosphorus is the asymmetric center. Various chiral phosphines PhP(R')R'' were synthesized for this purpose and stereoselectively introduced in the equatorial plane of octahedral complexes of the type $(MR(CO)_2L'(PMe_3)_2)^n$ ($n = 0$, L' = I, Br, Cl; $n = 1+$, L' = CO, NCMe, PR_3 (R = Me, CH_2Ph)) some of which were previously described.[1] An NMR study of these complexes was performed in order to establish whether the anisochrony expected for the diastereotopic PMe_3 axial ligands can be detected in their ^1H and ^{31}P spectra. Should the ^{31}P of these PMe_3 ligands be observed to be anisochronous, another point of interest would be the possibility of obtaining the values of trans and cis phosphorus–phosphorus coupling constants from ^{31}P spectra, since these complexes have three phosphorus ligands.

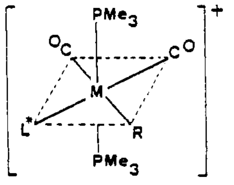

M = Fe, Ru.

1

Results

Synthesis of Asymmetric Phosphine Ligands. Asymmetric phosphorus ligands of various types have been synthesized in high yield by consecutive substitution of the two chlorine atoms of dichlorophenylphosphine in a one-pot reaction.[2]

$$PhPCl_2 \xrightarrow{I} PhP(R')Cl \xrightarrow{II} PhP(R')R''$$

In the first step, an organocadmium derivative R'_2Cd (R' = alkyl or aryl) was reacted at low temperature with $PhPCl_2$ to afford the corresponding chlorophosphine. Similarly, bulky alcohols or secondary amines led selectively to chloro esters (R' = OR) or chloro amides (R' = NR_2). In the second step, the remaining

---

[1] (a) Pańkowski, M. Bigorgne, M. *J. Organomet. Chem.* **1971**, *30*, 227. (b) Pańkowski, M. *Proc. Int. Conf. Coord. Chem. 16th, 1974*. (c) Pańkowski, M.; Bigorgne, M. *J. Organomet. Chem.* **1983**, *251*, 333.

[2] (a) Jore, D.; Guillerm, D.; Chodkiewicz, W. *J. Organomet. Chem.* **1978**, *149*, C7. (b) Chodkiewicz, W.; Guillerm, D.; Jore, D.; Mathieu, E.; Wodzki, W. *J. Organomet. Chem.* **1984**, *269*, 107.

0020-1669/85/1324-0533$01.50/0

chlorine atom was substituted, by using lithium or magnesium derivatives or alcohols.

Synthesis of Chiral Complexes. The asymmetric ligand L* was stereoselectively introduced into the equatorial plane of an octahedral complex in a cis orientation with respect to the R ligand by three different routes depending on the starting complex.

Method A. Treatment of $(MR(CO)_3(PMe_3)_2)^+A^-$ (**2**) with a phosphine L* in an organic polar solvent at low temperature (below −10 °C) yielded an acetyl derivative $(M(COR)(CO)_2L^*(PMe_3)_2)^+A^-$ (**3**), which lost CO on warming. This decarbonylation reaction gave the new alkyl dicarbonyl complex **1**, which was precipitated by addition of a nonpolar solvent.

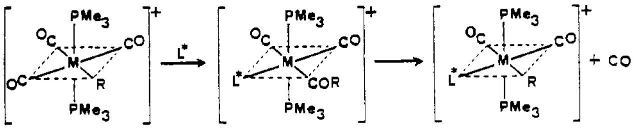

2 3 1

R = CH_3, CH_2Ph; L* = PhP(R′)R″

Method B. When a halogeno methyl complex $MXCH_3(CO)_2(PMe_3)_2$ (**4**) dissolved in methanol was allowed to react with an equimolar mixture of L* and $NaBPh_4$ between −30 and +20 °C, the final complex **1** was obtained as a crystalline precipitate while the NaX formed remained in solution. This reaction involves an unstable acetyl intermediate **5**, which could be isolated in some favorable cases if hexane were used instead of methanol, i.e. M = Fe, Ru and X = I.

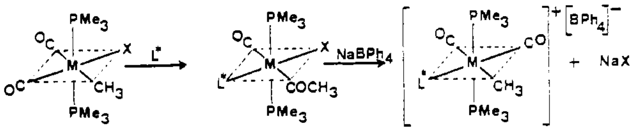

4 5 1

X = Cl, Br, I

Method C. When the starting complex used for the reaction with L* was $(MCH_3(CO)_2(NCMe)(PMe_3)_2)^+A^-$ (**6**), in a polar organic solvent between −30 and +20 °C, acetonitrile was easily substituted during the transformation of the probable intermediate **7** into **1**. The final chiral complex **1** was precipitated by addition of a nonpolar solvent.

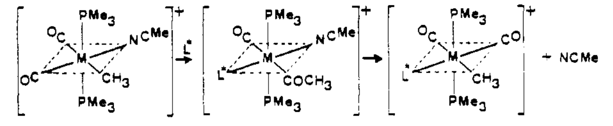

6 7 1

Due to the high reactivity of complexes **4** and **6** toward phosphine ligands, reactions B and C could be performed at −30 °C. Reaction at low temperature prevented a possible isomerization of the final complexes, which has been shown to occur with bulky L′ ligands.[3]

The chiral complexes were isolated in the solid state by precipitation at −30 °C. Their configurational stability in the solid state was sufficient to store them at ambient temperature. On the other hand, method A allowed the isolation and characterization of the acetylated intermediate **3**.

The reactions involved in methods A, B, and C share a common mechanism: the first step is the formation of an acetyl group by CO insertion into the metal–carbon σ-bond,[4] and the incoming phosphine ligand occupies a cis position relative to the acetyl group. The second step of method A is the decarbonylation of the acetyl intermediate **3**, which occurs on warming. This process is the reverse reaction of the cis CO insertion into the metal–carbon σ-bond so that L* remains cis with respect to the R ligand. In the case of methods B and C, because the ligands X or NCMe are very good leaving groups, the acetyl intermediates **5** and **7** are unstable and the decarbonylation process always gives isostructural complexes.

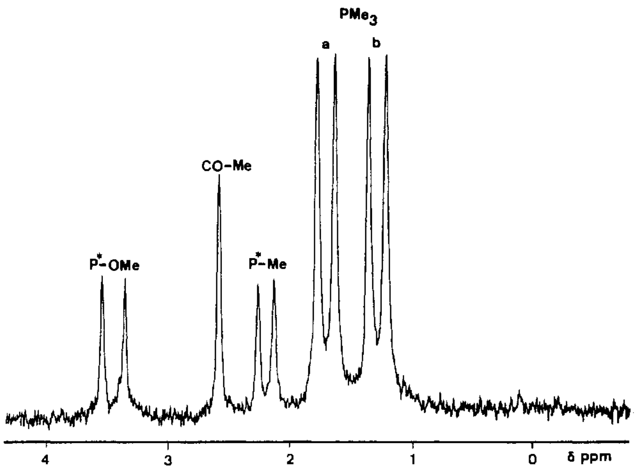

Figure 1. ^1H NMR spectrum (60 MHz, −20 °C) of $(Fe(COMe)(CO)_2(PhP(Me)(OMe))(PMe_3)_2)(ClO_4)$ in CD_2Cl_2 (high-field region).

Except for the iron complex containing the NCCH(Me)Cl ligand, all other complexes synthesized in this study contained a racemic phosphine L* = PhP(R′)R″, so that the asymmetric center was directly bonded to the metal: M = Fe, L* = NCCH(Me)Cl, PhP(Me)(*o*-C_6H_4OMe), PhP(Me)(CH_2Ph), PhP(Me)(Et), PhP(Me)(NEt_2), PhP(Me)(OMe), PhP(Me)(OPh), PhP(Me)(O-*t*-Bu); M = Ru, L* = PhP(OMe)(α-np), PhP(Me)(*o*-C_6H_4OMe), PhP(Me)(CH_2Ph), PhP(Me)(O-*t*-Bu), PhP(Me)(α-np) (α-np = α-naphthyl).

Chemical and Configurational Stability. Ruthenium complexes, whatever the equatorial phosphine ligand used, are generally stable in solution at ~30 °C for 1 day or more. On the other hand, the solution stabilities of iron complexes are strongly dependent on steric strain. If the equatorial ligand is small, L* = PhP(Me)(OR) or PhP(Me)(NEt_2), the solution stability of the Fe complexes is comparable to that of Ru complexes. But, in the case of bulky ligands such as PhP(Me)(CH_2Ph) or PhP(Me)(*o*-C_6H_4OMe), the Fe complexes in solution are stable only below −30 °C. Increasing the temperature results initially in their isomerization, which involves a permutation of L* with one of the trimethylphosphine ligands;[3] at higher temperature, some decomposition occurs with exchange of ligands and formation of byproducts, mainly $(FeCH_3(CO)_2(PMe_3)_3)^+A^-$.

When the equatorial ligand became very bulky, L* = PhP(Me)(α-np) or PhP(OMe)(α-np), the corresponding Fe complexes could not be obtained by using method A, B, or C while Ru complexes were successfully synthesized and were stable enough in solution at ~30 °C.

The singly acetylated iron complex of type **3** examined ($(Fe(COCH_3)(CO)_2L^*(PMe_3)_2)^+(ClO_4)^-$, L* = PhP(Me)(OMe)) was stable in solution below −10 °C (Figure 1). At higher temperature, this complex lost CO and gave $(FeCH_3(CO)_2L^*(PMe_3)_2)^+(ClO_4)^-$ (Figure 2).

IR Spectra. The IR spectra of complexes **1** and **3**, taken in methylene chloride in the CO stretching region, exhibit two strong bands with equal intensity. This is consistent with a molecule of C_1 symmetry but implies a cis orientation of the two CO ligands, as in structures **1**, **8**, **9**, or **10** (L = PMe_3).

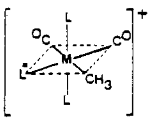
1 (*mer*)

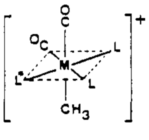
8 (*mer*)

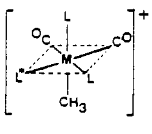
9 (*fac*)

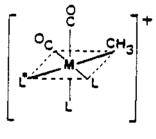
10 (*fac*)

No splitting attributable to the influence of the asymmetric center was observed. IR data do not allow the determination of

---

(3) Pańkowski, M.; Chodkiewicz, W.; Simonnin, M. P.; Pouet, M. J. *J. Chem. Soc., Chem. Commun.* **1981**, 1071.

(4) Pańkowski, M.; Bigorgne, M. Abstracts, VIIIth International Conference on Organometallic Chemistry, Kyoto, Japan, 1977.

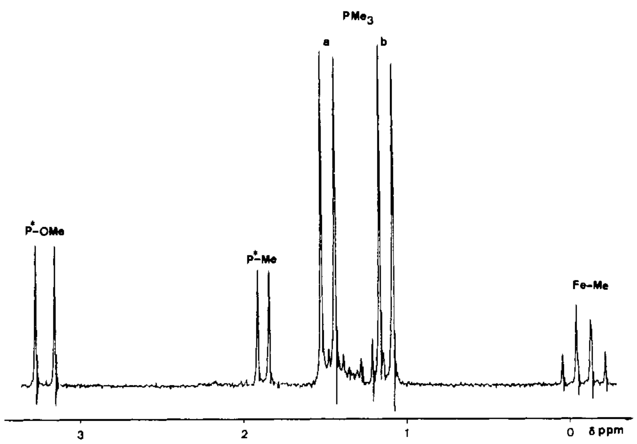

Figure 2. ^{1}H NMR spectrum (100 MHz) of $(FeMe(CO)_2(PhP(Me)(OMe))(PMe_2)_2)(ClO_4)$ in CD_2Cl_2 (high-field region).

the relative orientation of the phosphorus ligands, but this was achieved by an NMR study (vide infra).

The CO stretching frequencies are about 20 cm^{-1} higher for M = Ru than for M = Fe and are slightly dependent on the substituents bonded to the equatorial phosphorus (Tables I and II). The acetyl complex of type **3** exhibits another band of medium intensity at 1620 cm^{-1}, which is characteristic of an acetyl ligand bonded to a transition metal.

NMR Spectra. Complexes of C_s Symmetry. Before considering chiral complexes **1**, we shall first analyze a simpler case, i.e. octahedral complexes in which no asymmetric ligand is present in the equatorial plane: $(MCH_3(CO)_2L'(PMe_3)_2)^+A^-$ (M = Fe, Ru; L′ = CO, NCMe, PMe$_3$).

^{1}H NMR spectra of these complexes indicate that the two PMe$_3$ ligands are isochronous. This result requires the existence of a symmetry plane. Therefore, IR and NMR data are consistent only with structure **11** or **12**. When L′ = CO, or NCMe, the resonance of the methyl group bound to the metal is a triplet, which collapses to a singlet upon broad-band irradiation of the phosphorus. Hence the methyl ligand lies in the symmetry plane, and the spin–spin coupling with both phosphines, L, is equivalent. When L′ = PMe$_3$, a further doubling of this triplet is observed, indicating that the couplings with the ^{31}P nuclei in L and L′ are slightly different (Tables I and II).

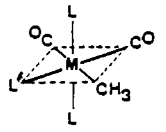

11 (*mer*)

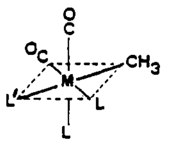

12 (*fac*)

The resonance of the isochronous PMe$_3$ ligands, which form an $X_9AA'X'_9$ system, gives a "filled-in" doublet[5] for M = Ru and Fe. This "filled-in" doublet consists of a sharp doublet (*N* doublet) and a broadened central band. Harris[6] has shown that the *N* doublet is symmetrically disposed about ν_X and its splitting is $N = |J_{AX} + J_{AX'}|$; half of the total intensity lies in this *N* doublet. The appearance of the whole X spectrum is dependent on $|J_{AA'}|$; $L = |J_{AX} - J_{AX'}|$ and $N = |J_{AX} + J_{AX'}|$. An apparent triplet is observed when $|J_{AA'}| \gg L$, but if L is nonzero and small, the central band of this apparent triplet may appear broader than the two outer lines. Obviously, the observation of a "filled-in" doublet does not require a trans orientation of the PMe$_3$ ligands.

An unambiguous distinction between structures **11** and **12** can be made by ^{13}C NMR as the two carbonyl ligands are equivalent in **12** but inequivalent in **11**. The ^{13}C spectra of iron complexes with L′ = P(OMe)$_3$ and PMe$_3$ exhibit two distinct signals at very low field ($\delta > 200$) as expected for carbonyl ligands. Each of these signals is a doublet of triplets for L′ = P(OMe)$_3$, and both J_{PC} values have similar magnitude for the less deshielded ^{13}CO, which is cis to the three phosphorus ligands. Quite different J_{PC} values are observed for the most deshielded ^{13}CO, which is cis to the two PMe$_3$ ligands but trans to P(OMe)$_3$; i.e. ${}^2J_{PC}{}^{trans} > {}^2J_{PC}{}^{cis}$.[7] When L′ = PMe$_3$ the low-field ^{13}CO signal is also a doublet of triplets with unequal J_{PC} values while the less deshielded ^{13}CO signal is a quadruplet, as expected for a CO ligand with three PMe$_3$ ligands in cis positions. Therefore, ^{13}C NMR data (Table III) are consistent only with structure **11**.

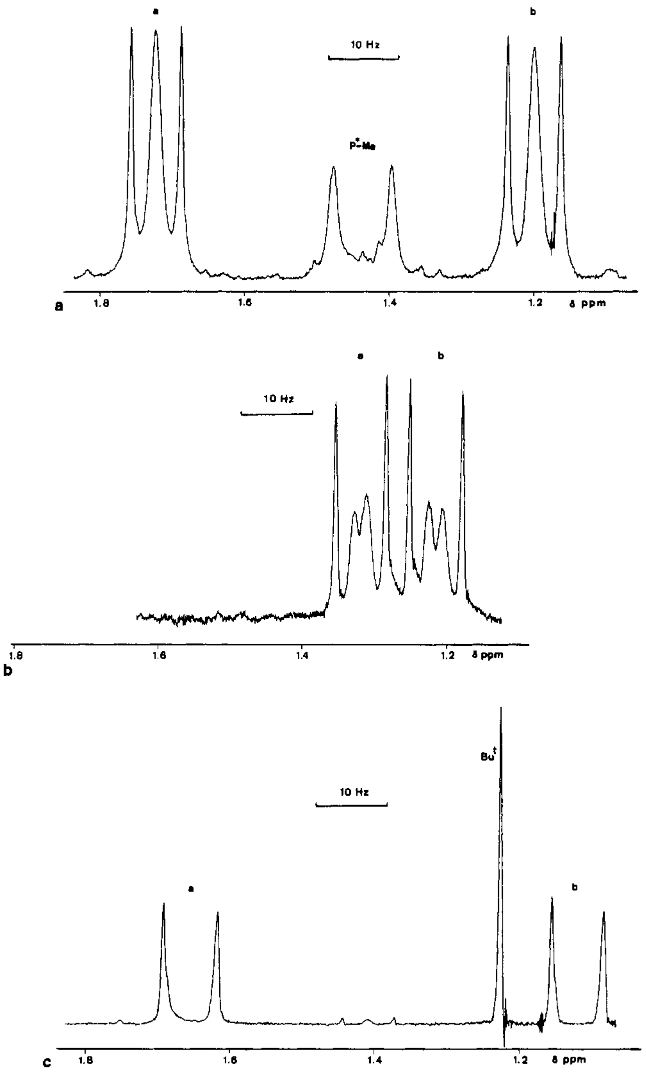

Figure 3. ^{1}H NMR spectra (100 MHz) of $(RuMe(CO)_2L^*(PMe_3)_2)(BF_4)$ in CD_2Cl_2 (resonances of the diastereotopic PMe$_3$ groups): (a) L* = PhP(Me)(CH$_2$Ph); (b) L* = PhP(Me)(o-C$_6$H$_4$OMe); (c) L* = PhP(Me)(O-t-Bu).

In agreement with the ^{1}H and ^{13}C NMR results, ^{31}P NMR spectra of Fe and Ru complexes **11** with L′ = PMe$_3$ are of the A_2B type and allow the cis coupling $^2J_{PP}$ to be determined (Table IV).

Complexes of C_1 Symmetry. As expected, when the equatorial ligand is chiral, the ^{1}H NMR spectra of complexes **1** show that the axial PMe$_3$ groups become diastereotopic and give two distinct resonances (Tables I and II). These resonances are very close when L* = NCCH(Me)Cl (M = Fe) and the "filled-in" doublets strongly overlap, but their separation increases with the observing frequency (100 and 250 MHz). Two well-separated "filled-in" doublets are observed when L* = PhP(Me)(CH$_2$Ph) (M = Fe,

---

(5) Redfield, D. A.; Nelson, J. H.; Cary. L. W. *Inorg. Nucl. Chem. Lett.* **1974**, *10*, 727.

(6) (a) Harris, R. K. *Can. J. Chem.* **1964**, *42*, 2275. (b) Harris, R. K.; Hayter, R. G. *Can. J. Chem.* **1964**, *42*, 2282. (c) Finer, E. G.; Harris, R. K. *Mol. Phys.* **1967**, *12*, 457.

(7) Gansow, D. A.; Kimura, B. Y.; Dobson, G. R.; Brown, R. A. *J. Am. Chem. Soc.* **1971**, *93*, 5922.

Table I. IR and ^{1}H NMR Data[a] for $(FeR(CO)_2L'(PMe_3)_2)(BPh_4)$ Complexes

		Fe–R				PMe_3(a)		PMe_3(b)			L′		
L′	IR ν_{CO}, cm^{-1} (s, A′)	R	δ	$^3J_{P_{ax}H}$	$^3J_{P_{eq}H}$	δ_a	N_a	δ_b	N_b	$\Delta\delta$	R′/R″	δ	J
CO	*b*	Me	+0.05 (t)	7.2		1.56	9.1						
NCMe[c]	2020.0, 1965.0	Me	+0.23 (t)	8.5		1.49	8.8				NCMe	1.69	$^5J_{PH} = 2.3$
py	2022.0, 1966.0	Me	+0.48 (t)	8.0		1.27	8.2						
PMe_3	2018.0, 1961.0	Me	−0.16 (d × t)	8.1	10.3	1.55	7.9				Me	1.45	$^2J_{PH} = 8.0$
$P(OMe)_3$	2025.0, 1970.0	Me	−0.09 (d × t)	8.1	9.4	1.50	8.6				OMe	3.75	$^3J_{PH} = 10.8$
NCCH(Me)Cl[d]	2020.0, 1965.0	Me	+0.26 (t)	8.3		1.52	8.6	1.51	8.6	0.01	CH Me	4.25 1.60	$^3J_{PH} = 7.0$
PhP(*o*-C_6H_4OMe)(Me)[e]	2022.1, 1966.0	Me	+0.05 (q)	8.8	8.8	1.46	8.0	1.38	8.0	0.08	Me OMe	2.25 3.98	$^2J_{PH} = 8.0$
PhP(CH_2Ph)(Me)[e]	2016.0, 1959.0	Me	−0.03 (q)	8.7	8.7	1.57	7.8	1.20	7.8	0.37			
PhP(Me)(Et)[e]	2013.0, 1957.0	Me	−0.08 (d × t)	8.6	9.2	1.41	8.0	1.21	8.0	0.20	Me CH_2CH_3	1.59 0.86	$^2J_{PH} = 8.3$ $^3J_{PH} = 14.4$ $^3J_{HH} = 7.2$
PhP(Me)(NEt_2)	2023.0, 1965.0	Me	−0.10 (d × t)	8.4	9.1	1.51	8.5	1.13	8.3	0.38	Me CH_2CH_3	1.91 1.22	$^2J_{PH} = 7.2$ $^3J_{HH} = 7.0$
PhP(Me)(OMe)	2023.0, 1967.0	Me	−0.09 (d × t)	8.5	9.3	1.48	8.4	1.13	8.3	0.35	Me OMe	1.88 3.22	$^2J_{PH} = 7.0$ $^3J_{PH} = 11.7$
PhP(Me)(OPh)	2025.0, 1970.0	Me	+0.06 (d × t)	8.3	9.7	1.60	8.5	1.19	8.3	0.41	Me	2.04	$^2J_{PH} = 6.4$
PhP(Me)(O-*t*-Bu)	2025.0, 1968.0	Me	−0.02 (d × t)	8.5	9.3	1.57	8.7	1.14	8.4	0.43	Me O-*t*-Bu	2.11 1.26	$^2J_{PH} = 7.2$
PhP(Me)(OMe)[e,f]	2023.0, 1975.0	C=O(Me)	2.56 (s)			1.69	8.8	1.27	8.4	0.42	Me OMe	2.18 3.43	$^2J_{PH} = 7.7$ $^3J_{PH} = 11.3$

[a] Chemical shifts relative to internal Me_4Si. *J* and *N* values in hertz. Solvent CD_2Cl_2/CH_2Cl_2. [b] $\nu_{CO} = 2084.0$ (w, A_1), 2021.0 (vs, $A_1 + B_1$) cm^{-1}. [c] $\nu_{C\equiv N} = 2287.0$ (w, A_1) cm^{-1}. [d] $\nu_{C\equiv N} = 2272.0$ (w, A_1) cm^{-1}. [e] At −20 °C. [f] Anion = $(ClO_4)^-$; $\nu_{C=O(Me)} = 1620$ (m) cm^{-1}.

Table II. IR and ^{1}H NMR Data[a] for $(Ru(CO)_2L'(PMe_3)_2)(BF_4)$ Complexes

		Ru–R				PMe_3(a)		PMe_3(b)			L′		
L′	IR ν_{CO}, cm^{-1} (s, A′)	R	δ	$^3J_{P_{ax}H}$	$^3J_{P_{eq}H}$	δ_a	N_a	δ_b	N_b	$\Delta\delta$	R′/R″	δ	J
CO	*b*	Me[c]	−0.06 (t)	6.8		1.88	8.2						
NCMe	2045.0, 1987.0	Me	−0.14 (t)	7.7		1.58	7.5				NCMe	2.44	$^5J_{P_{ax}H} = 1.6$
PPh_3	2046.0, 1987.0	Me	−0.55 (q)	8.1	8.1	1.37	7.0						
PMe_3	2046.0, 1987.0	Me	−0.42 (d × t)	7.8	8.2	1.62	6.8				Me	1.54	$^2J_{PH} = 8.1$
PhP(OMe)(α-np)	2045.0, 1988.0	Me	−0.26 (q)	7.4	7.4	1.35	7.3	1.32	7.4	0.03	OMe	3.03	$^3J_{PH} = 11.6$
PhP(*o*-C_6H_4OMe)(Me)	2047.0, 1986.0	Me	−0.30 (t × d)	7.9	7.2	1.32	7.0	1.22	7.3	0.10	Me OMe	2.03 3.74	$^2J_{PH} = 7.5$
PhP(Me)(CH_2Ph)	2042.0, 1985.0	Me	−0.29 (t × d)	8.0	7.4	1.73	6.9	1.21	7.3	0.52	Me CH_2Ph(AB)	1.44 3.50 3.21	$^2J_{PH} = 8.0$ $^2J_{PH_A} = 6.25$ $^2J_{PH_B} = 1.55$ $^2J_{H_AH_B} = -14.4$
PhP(Me)(O-*t*-Bu)	2046.0, 1988.0	Me	−0.32 (t × d)	8.0	7.4	1.66	7.5	1.12	7.2	0.54	Me O-*t*-Bu	2.19 1.23	$^2J_{PH} = 7.1$
PhP(Me)(α-np)[d]	2045.0, 1937.0	Me	−0.19 (q)	7.9	7.9	1.55	7.0	0.85	7.0	0.70	Me	2.15	$^2J_{PH} = 7.6$
PhP(Me)(O-*t*-Bu)	2045.0, 1986.0	CH_2Ph	2.1	*e*	*e*	1.60	7.3	1.13	7.1	0.47	Me O-*t*-Bu	2.27 1.28	$^2J_{PH} = 7.0$

[a] Chemical shifts relative to internal Me_4Si. *J* and *N* in hertz. Solvent CD_2Cl_2/CH_2Cl_2. [b] $\nu_{CO} = 2116.0$ (w, A_1), 2043.0 (vs, $A_1 + B_1$) cm^{-1}. [c] Solvent $(CD_3)_2CO$. [d] Anion = $(BPh_4)^-$. [e] Complex pattern.

Table III. ^{13}C NMR Data[a] for $(FeCH_3(CO)_2L'(PMe_3)_2)(BPh_4)$ Complexes

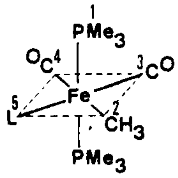

	C_1		C_2			C_3			C_4			C_5	
L'	δ_{C_1}	N	δ_{C_2}	$^2J_{P_1C_2}$	$^2J_{P_5C_2}$	δ_{C_3}	$^2J_{P_1C_3}$	$^2J_{P_5C_3}$	δ_{C_4}	$^2J_{P_1C_4}$	$^2J_{P_5C_4}$	δ_{C_5}	$J_{P_5C_5}$
$P(OMe)_3$[b]	18.0	31.9	−10.1	14.9	24.5	213.4	25.3	73.8	206.8	16.7	27.8	55.4	10.8
PMe_3[c]	18.6	29.9	−7.8	16.6	16.6	213.9	27.9	41.3	207.3	18.4	18.4	17.9	28.3

[a] Chemical shifts relative to internal Me_4Si. J and N values in hertz. Solvent CD_2Cl_2. [b] At 25.17 MHz. [c] At 62.8 MHz.

Table IV. ^{31}P NMR Data[a] for Fe and Ru $(MR(CO)_2L'(PMe_3)_2)$ Anion Complexes

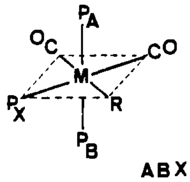

ABX

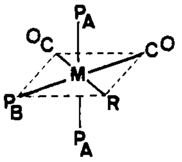

A_2B

M	L'	R	anion	spectrum type	δ_{P_X}	δ_{P_A}	δ_{P_B}	$^2J_{P_AP_B}{}^{trans}$	$^2J_{P_AP_X}{}^{cis}$	$^2J_{P_BP_X}{}^{cis}$
Fe	PMe_3	Me	BPh_4^-	A_2B	9.1	13.8			65.1	
Fe	PhP(Me)(OMe)	Me	BPh_4^-	ABX	154.4	12.3	9.9	83.8	71.8	64.2
Fe	PhP(Me)(O-*t*-Bu)	Me	BPh_4^-	ABX	138.6	11.5	8.1	89.1	71.6	63.8
Fe	$PhP(Me)(NEt_2)$	Me	BPh_4^-		150.1[b]	11.8[b]	9.0[b]			
Ru	PMe_3	Me	BF_4^-	A_2B	−16.4	−14.3			39.1	
Ru	$PhP(Me)(o\text{-}C_6H_4OMe)$	Me	BF_4^-	AB_2	−5.1	−16.1			38.9	
Ru	PhP(Me)(O-*t*-Bu)	Me	BF_4^-	ABX	113.6	−13.1	−17.3	222.2	36.6	36.6
Ru	PhP(Me)(O-*t*-Bu)	CH_2Ph	BPh_4^-	ABX	110.6	−16.1	−20.2	219.1	36.0	36.0

[a] Chemical shifts relative to external H_3PO_4 (85%). Positive δ values are in the direction of increasing frequency. J values in hertz. Solvent CH_2Cl_2/CD_2Cl_2. [b] δ values determined by $^1H\{^{31}P\}$ double-resonance experiments.

Ru), showing that the ^1H NMR spectra are second order in both cases (Figure 3a).

For Ru complexes two interesting cases were observed when L* = $PhP(Me)(o\text{-}C_6H_4OMe)$ and PhP(Me)(α-np): in both cases the "filled-in" doublets consist of a sharp doublet (N doublet) and two broad inner bands (Figure 3b). Even though these resonances have similar patterns, it must be noted that they are close together for L* = $PhP(Me)(o\text{-}C_6H_4OMe)$ but well separated for L* = PhP(Me)(α-np). This indicates that the observed doubling of the inner band is not related to the magnitude of ^1H inequivalence.

On the other hand, the "filled-in" doublets change into two well-separated doublets without the central band when L* = PhP(Me)(O-*t*-Bu) (M = Fe, Ru), suggesting that the ^1H NMR spectra become approximately first order (Figure 3c).

Whatever the pattern of the "filled-in" doublets, they collapse to two equally intense singlets under ^{31}P noise decoupling conditions, which confirms that the two PMe_3 axial ligands are anisochronous.

For some characteristic complexes, which are stable at about 30 °C, ^{31}P spectra with proton noise decoupling were studied at 32.4 MHz, at ambient temperature (Table IV). ABX spectra were observed for L* = PhP(Me)(OMe) (M = Fe) and L* = PhP(Me)(O-*t*-Bu) (M = Fe, Ru). Therefore, the ^{31} P nuclei of the axial PMe_3 ligands are anisochronous, as observed for proton resonance (first-order spectra). Moreover, the magnitude of the P–P coupling constants obtained by analysis of the ABX spectra confirms the trans orientation of the PMe_3 ligands in agreement only with structure **1**.

In the case of the Ru complex with L* = $PhP(Me)(o\text{-}C_6H_4OMe)$, the ^{31}P spectrum appeared to be of the AB_2 type, which indicates that the ^{31}P nuclei of the axial PMe_3 ligands seem to be isochronous at this observing frequency. In this particular case, inequivalence was observed in the 100-MHz proton spectrum but this was second order.

Correlation of ^1H and ^{31}P NMR spectra was achieved by selective ^{31}P irradiation. When L* = PhP(Me)(OR) (M = Fe, Ru) and L* = $PhP(Me)(NEt_2)$ (M = Fe), the ^1H doublets of the axial PMe_3 ligands were well separated and different ^{31}P irradiation frequencies were necessary to collapse each doublet into a singlet. The ^{31}P irradiation frequencies indicate that ^1H and ^{31}P inequivalences are of the same sign; i.e., the more shielded protons are associated with the more shielded phosphorus.

Similar $^1H\{^{31}P\}$ selective irradiations indicate that the ^{31}P resonance of the L* ligand is strongly deshielded. ^{31}P chemical shifts calculated from irradiation frequencies[8,9] are in very good agreement with δ values obtained directly from ^{31}P NMR spectra.

Computer Simulation of Proton Spectra. Knowledge of J_{PP} in ruthenium complexes gives the opportunity to perform computer simulations of proton spectra, in order to test the influence of the various parameters on the appearance of the whole spectrum.

A simulated $X_9AA'X'_9$ spectrum identical with the experimental "filled-in" doublet observed for L' = NCMe was obtained only with J_{AX} and $J_{A'X}$ of opposite signs: $J_{AX} = \pm 8.2$, $J_{AX'} = \mp 0.7$, $|J_{AA'}| = 222.2$ Hz. These J values were kept constant, and further simulations were performed to examine first the influence of proton inequivalence ($X_9AA'Y_9$ spectra) and then the influence of both ^1H and ^{31}P inequivalence (X_9ABY_9 spectra) on the shape of the proton spectra.

Simulated spectra showed two "filled-in" doublets with a single central band if $\nu_A = \nu_{A'}$ and $\nu_X \neq \nu_Y$ with $\nu_X - \nu_Y$ varying from 50 to 100 Hz. Splitting of the inner broad band was observed when both ^1H and ^{31}P were taken inequivalent ($\nu_X \neq \nu_Y$, $\nu_A \neq \nu_B$), and the separation between these broad inner bands increased with ^{31}P inequivalence (Figure 4).

---

(8) Mc Farlane, W. *Proc. R. Soc. London, Ser. A.* **1968**, *306*, 185.
(9) Lequan, R. M.; Pouet, M. J.; Simonnin, M. P. *Org. Magn. Reson.* **1975**, *7*, 392.

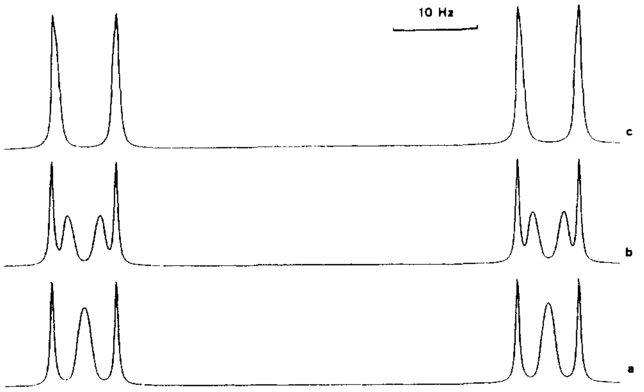

Figure 4. Simulated ^{1}H spectra (XY part) of X_9ABY_9 systems with $\nu_X - \nu_Y = 54$ Hz, $J_{AB} = 222.2$ Hz, $J_{AX} = +8.2$ Hz, $J_{AY} = -0.7$ Hz, $J_{BX} = -0.7$ Hz, $J_{BY} = +7.9$ Hz, and $J_{XY} = 0$: (a) $\nu_A - \nu_B = 10$ Hz; (b) $\nu_A - \nu_B = 100$ Hz; (c) $\nu_A - \nu_B = 250$ Hz. Splitting of the central band in each *N* doublet is observed in case b.

These simulations indicate that the presence of two inner bands in each of the "filled-in" doublets imply phosphorus inequivalence. The experimetnal proton spectrum observed at 100 MHz for the Ru complex with L* = PhP(Me)(o-C_6H_4OMe) exhibits two "filled-in" doublets each having two inner bands (Figure 3b); although the ^{31}P spectrum of this complex seems to be of the AB_2 type at 32 MHz, the ^{31}P nuclei of the axial PMe_3 ligands are certainly slightly inequivalent at 40.5 MHz.

Discussion

The CO stretching frequencies of metal carbonyl complexes with one or several phosphorus ligands are known to depend on the substituents bonded to phosphorus.[10,11] This has been related to the extent of σ and π transfer between the transition metal and phosphorus. IR data obtained here for Fe and Ru complexes **1** (Tables I and II) indicate that these frequencies are almost constant in each series. This suggests that, for a given metal, the character of the metal–phosphorus bond is very similar.

The ^{1}H NMR data for the axial PMe_3 ligands (Tables I and II) indicate that inequivalence is very small when the asymmetric center is far removed; e.g. in the linear fragment Fe—N≡C—CH(Me)Cl, it is in the γ position relative to the metal and the inequivalence is only $\Delta\delta = 0.01$. When the equatorial ligand L* is a chiral phosphine, the asymmetric center is directly bonded to the metal and the magnitude of the inequivalence is strongly dependent on the substitutents on phosphorus. It must be noted that the presence of a strongly anisotropic substituent such as α-naphthyl does not necessarily induce an important inequivalence since for M = Ru, $\Delta\delta$ is small when L* = PhP(OMe)(α-np) but is the greatest observed when L* = PhP(Me)(α-np). This strongly suggests that the conformation about the M–P* bond plays an important role.

Substituents are either staggered or eclipsed during rotation around a bond joining two tetrahedral atoms, but a similar situation does not exist when a tetrahedral center rotates relative to a tetragonally coordinated transition metal. In our case, the tetragonal coordination plane comprises the two trans PMe_3 ligands, the methyl ligand, and one CO ligand; the remaining CO ligand is out of this plane and need not be considered.

If the tetrahedral center is asymmetric, two pairs of 12 possibilities can theoretically exist. Six involve eclipsing between one of the phosphorus substituents and one of the two PMe_3 ligands, three involve eclipsing between one of the phosphorus substituents and the CO ligand, and three involve eclipsing between one of the phosphorus substituents and the methyl group.

Examination of molecular models suggests that possible conformers are close to these ideal representations but are slightly staggered to avoid steric interactions that would arise from perfect eclisping; in all cases, only one phosphorus substituent lies above and two lie below the equatorial plane, as shown in Chart I, where the projection is made along the P*–M bond.

Chart I

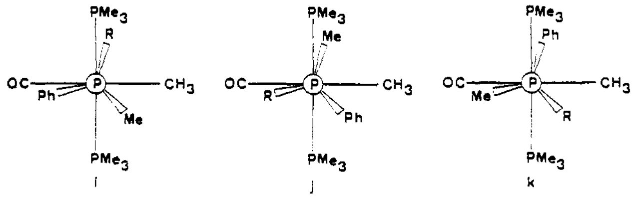

Although the observed chemical shifts are weighted averages of the corresponding chemical shifts in the individual conformers, experimental proton shifts for the methyl group bonded to the metal and for the diastereotopic axial PMe_3 groups allow the predominant spatial environment of these ligands to be deduced.

Preliminary information about the conformation may be deduced from the proton shift of the methyl bonded to the metal. When going from L′ = PMe_3 to an asymmetric phosphine L*, this resonance is shifted to low field in all the Fe and Ru complexes examined. This trend, which is opposite to that observed in Ru complexes **11** when L′ = PMe_3 ($\delta_{Me} = -0.42$) is replaced by L′ = PPh_3 ($\delta_{Me} = -0.55$), allows the exclusion of conformation(s) in which an aryl substituent would be in the vicinity of this methyl ligand.

Much information may be obtained from the individual chemical shifts of the diastereotopic PMe_3 ligands and from the magnitude of their inequivalence. When L* = PhP(Me)(o-C_6H_4OMe), the proton inequivalence is small (M = Fe, $\Delta\delta = 0.08$; M = Ru, $\Delta\delta = 0.10$) and both signals show higher shielding than those in similar complexes with L′ = PMe_3 but close to that observed for L′ = PPh_3 (M = Ru). This can be explained by a favored conformation of type k in which each PMe_3 ligand is in the vicinity of an aryl substituent. This type of conformation explains also that the ^{31}P nuclei of these axial ligands seem to be isochronous in the Ru complex. A similar conclusion holds for L* = PhP(OMe)(α-np) (M = Ru).

Quite different results are found for the Ru complex with L* = PhP(Me)(α-np) where the proton inequivalence is the greatest observed ($\Delta\delta = 0.70$) and where one PMe_3 signal remains near that observed for L′ = PMe_3 while the other is strongly shielded. A favored conformation of type j, where one PMe_3 is located near the Me substituent and the other PMe_3 is in the vicinity of two strongly anisotropic aryls, can explain these data. Therefore, conformations of types j and k are favored when two of the P* substituents are very bulky (Ph, o-C_6H_4OMe, α-np).

Coexistence of the three types of conformation (i, j, and k) can be deduced from experimental shifts obtained for the Fe complex with L* = PhP(Me)(Et) as the inequivalence is relatively small ($\Delta\delta = 0.20$) and both signals are somewhat shielded relative to that observed for L′ = PMe_3.

Conformations of type i should become more probable when the bulkiness of L* decreases. The experimental data for the Fe complex with L* = PhP(Me)(OMe) and L* = PhP(Me)(OPh) and for the Fe and Ru complexes with L* = PhP(Me)(O-t-Bu) show that, in these four cases, the low-field PMe_3 signals are near that observed for L′ = PMe_3 or L′ = $P(OMe)_3$ (M = Fe), while the upfield PMe_3 signals are among the more shielded in the absence of an α-naphthyl substituent. Such results are compatible with favored conformations of type i or j. A large inequivalence is also observed in the ^{31}P spectra for three of these complexes (M = Ru, $\Delta\delta_{^{31}P} = 4.1$; M = Fe, $\Delta\delta_{^{31}P} = 3.4$). This suggests that the axial phosphorus atoms have quite different environments and that a conformation of type i is favored. This hypothesis is further supported by the proton chemical shifts observed in the Fe complex with L* = PhP(Me)(OMe): the low-field PMe_3 signal is very close to that observed for L′ = $P(OMe)_3$. A similar situation seems to prevail in the Fe complex with L* = PhP(Me)(NEt_2).

Stabilization of the i type conformation for small ligands such as L* = PhP(Me)(OR) and PhP(Me)(NEt_2) could be explained either by a dipolar interaction between a partially negatively charged oxygen and a partially positively charged phosphorus[12a]

---

[10] Bigorgne, M. *J. Inorg. Nucl. Chem.* **1964**, *26*, 107.
[11] Tolman, C. A. *J. Am. Chem. Soc.* **1970**, *92*, 2953.

or by through-space 2p–3d overlap effects between a methoxy[12b] or an amino group and the axial phosphorus.

Many determinations of phosphorus–phosphorus coupling constants in transition-metal complexes have led workers to emphasize the importance of such data to determine the relative orientation of the phosphorus ligands.[13] However many other factors are known to strongly influence the magnitude of $^2J_{PP}$,[14] e.g. the nature of the transition metal, the ligands other than phosphorus in the complex, and the substituents bonded to the phosphorus, especially when atoms of different electronegativities are involved.

Different methods can be used to obtain $^2J_{PP}$ in a complex containing two chemically equivalent phosphorus ligands, such as (a) observation of the weak-intensity wing peaks, (b) computer simulation of the ^{1}H band shape, or (c) ^{1}H{^{31}P} NMR double-resonance experiments.[6,15]

Computer simulation of the band shape gives only approximate values of $|^2J_{PP}|$ which, in some cases, have been found to agree poorly with data obtained by other methods.[15b] Obviously, the ^{31}P spectrum does not give $^2J_{PP}$ since the two ^{31}P nuclei are isochronous.

Octahedral Fe and Ru complexes $(MR(CO)_2L'(PMe_3)_2)^+A^-$ with three phosphorus ligands (structure **11**) have C_s symmetry. Their ^{31}P spectra are of the A_2B type and give only $|J_{AB}| = |^2J_{PP}{}^{cis}|$. When L′ = PMe_3, analysis of the ^{31}P spectra gives $|^2J_{PP}{}^{cis}| = 39$ Hz for M = Ru and $|^2J_{PP}{}^{cis}| = 65$ Hz for M = Fe.

Replacement of L′ = PMe_3 by an asymmetric phosphorus ligand L* removes the symmetry plane, and ^{31}P spectra of the ABX type are expected if ^{31}P inequivalence is not too small. ^{31}P spectra of the ABX type are observed when one of the substituents of the asymmetric phosphine is an alkoxy group. For the Ru complex with P* = PhP(Me)(O-*t*-Bu) and R = Me, the two high-field P_A and P_B nuclei of the PMe_3 ligands are found to be strongly coupled: $|J_{AB}| = 222.2$ Hz, in agreement with their trans orientation. The low-field P_X nucleus is weakly coupled to P_A and P_B: $|J_{AX}| = |J_{BX}| = 36.6$ Hz, as expected for cis coupling. Replacing R = Me by R = CH_2Ph has only a minor influence on these coupling constants. The magnitude of $^2J_{PP}{}^{trans}$ is in agreement with literature data.[13]

^{31}P spectra of two iron complexes with L* = PhP(Me)(OMe) and L* = PhP(Me)(O-*t*-Bu) were examined and gave very similar results. Analysis of the ABX spectra indicates that the asymmetric phosphorus P_X is unequally coupled to each of the axial P_A and P_B phosphorus atoms and that J_{AX} and J_{BX} have the same sign. Here also, the magnitude of $^2J_{PP}{}^{trans}$ is greater than $^2J_{PP}{}^{cis}$.

The observation of two equal cis P–P couplings for M = Ru but two unequal couplings for M = Fe can be ascribed to bond angle deformations due to greater strain for M = Fe than for M = Ru as the covalent radius increases from Fe to Ru.

Comparison of $^2J_{PP}$ in our Fe and Ru octahedral complexes with the same ligands shows that the absolute values of $^2J_{PP}{}^{trans}$ increase while those of $^2J_{PP}{}^{cis}$ decrease on descending the group. A similar trend has been observed[14,15] in *trans*-$M(CO)_4(PR_3)_2$ with M = Cr and Mo ($^2J_{PP}{}^{trans} = -15$ and $+162$ Hz, respectively): a strong increase is observed on descending the group. Similarly, $^2J_{PP}{}^{cis}$ increases in *cis*-$M(CO)_4(P(OMe)_3)$ for *M* = Cr ($J = -36$ Hz), Mo ($J = -29.7$ Hz), and *W* ($J = -25$ Hz).

The strong increase in $|^2J_{PP}{}^{trans}|$ observed from Fe to Ru compared to that reported in the case of Cr and Mo suggests that $^2J_{PP}{}^{trans}$ is positive in the Ru complexes. Similar considerations suggest that $^2J_{PP}{}^{cis}$ is negative in the Fe complexes examined.

Conclusion

It has been shown that the presence of an asymmetric center directly bonded to the metal of octahedral complexes, **1**, results in the anisochrony of the identical PMe_3 groups. The degree of the proton inequivalence is related to the conformation of the asymmetric group relative to the other ligands.

In some favorable cases where the asymmetric center is a phosphorus atom bearing an alkoxy or an amino substituent, axial phosphorus ligands become strongly inequivalent. In such cases, and for the first time, ^{31}P NMR allows a direct determination of cis and trans phosphorus–phosphorus coupling constants in transition-metal complexes. The geometrical relationship of phosphorus ligands can be unequivocally deduced from the inequality $|^2J_{PP}{}^{trans}| > |^2J_{PP}{}^{cis}|$.

For Ru complexes, the trans $^2J_{PP}$ is much greater than the cis one, while for the Fe complexes, this difference is much smaller so that knowledge of only one of these coupling constants is not sufficient to deduce the configuration of iron complexes.

Furthermore, this study indicates that the two series of octahedral Fe and Ru complexes prepared by the same chemical reactions have the same geometrical configuration.

Experimental Section

All manipulations were carried out under an inert atmosphere of N_2 or Ar by using standard procedures. Solvents were purified by standard methods.

IR and NMR Spectra. IR spectra were recorded on a Perkin-Elmer 221 spectrometer (solvent CH_2Cl_2) using a 0.5-mm CaF_2 cell.

^{1}H NMR spectra were recorded at either 60 MHz (Varian A60, T60), 100 MHz (Varian XL-100-12 WG, CW mode, 5-mm tubes), or 250 MHz (Cameca, FT mode, 5-mm tubes). The ^{1}H resonance of the solvent (CH_2Cl_2/CD_2Cl_2) was used to provide the field frequency lock at 100 MHz. Heteronuclear ^{1}H{^{31}P} double-resonance experiments were performed by irradiating the ^{31}P nuclei at 40.5 MHz with the XL gyrocode decoupler. The ^{31}P irradiation frequency was determined with an Eldorado-Varian frequency counter, and ^{31}P chemical shifts relative to H_3PO_4 (85%) were calculated as previously described.[9,16]

^{13}C spectra with ^{1}H noise decoupling were recorded at 25.17 MHz (Varian XL-100) or 62.86 MHz (Bruker WM.250) (FT mode, 10-mm tubes) by using the solvent ^{2}H signal for an internal field frequency lock.

^{31}P spectra with ^{1}H noise decoupling were recorded at 32.4 MHz on a Bruker WP.80 instrument (FT mode, 10-mm tubes), by using the solvent (CH_2Cl_2/CD_2Cl_2) ^{2}H signal for an internal field frequency lock. ^{31}P chemical shifts were calculated relative to external H_3PO_4 (85%).

Simulations of the $X_9AA'X'_9$ and X_9ABY_9 spin systems were performed on an ASPECT 2000 system using the PANIC simulation program.

Preparation of Asymmetric Phosphorus(III) Ligands PhP(R′)R″. Step I. All reactions started with 0.05 mol of dichlorophenylphosphine (6.75 mL) dissolved in ether (25 mL).

A. Chlorophosphines PhP(R′)Cl (R′ = Me, *α*-np). The organocadmium derivative R'_2Cd (0.025 mol), prepared in ca. 0.5 M solution in ether (or ether/THF for R′ = Me), was added dropwise to the stirred dichlorophenylphosphine solution at −76 °C.[2] The reaction mixture was then allowed to come slowly to room temperature.

B. Phosphinous Chloro Ester and Chloro Amide PhP(R′)Cl (R′ = O-*t*-Bu, NEt_2). Triethylamine (7.5 mL) was added to the stirred dichlorophenylphosphine solution at −76 °C, followed by dropwise addition of *tert*-butyl alcohol (4.7 mL, 0.05 mol) or diethylamine (5.2 mL, 0.05 mol), in ether/pentane (125 mL, 1:4). The reaction mixture was then warmed slowly to room temperature.

Step II. A. Tertiary Phosphines (R′ = Me; R″ = *o*-C_6H_4OMe, CH_2Ph, *α*-np). A slight excess (ca. 10%) of a Grignard solution of R″MgX was added to the stirred reaction mixture obtained from step IA, at −20 °C. The resulting mixture was then allowed to come to room temperature and either 30% aqueous acetic acid (15 mL) for R″ = CH_2Ph and *α*-np or 50% aqueous potassium cyanide solution (20 mL) for R″ = *o*-C_6H_4OMe was added. The organic layer was separated and washed with water. The solvent and the dimethylphenylphosphine, occasionally formed in step IA, were removed under vacuum and condensed in a cold trap. The residue was treated with ether (5 mL) and pentane (45 mL) and allowed to stand for 24 h, after which the clear solution was separated from a little gummy resin and the solvent was removed under vacuum. The products were obtained as oily liquids that solidified slowly at room temperature. Average yields: 85 ± 5%.

The tertiary phosphines were characterized by ^{1}H NMR (Varian T 60) in $CDCl_3$: PhP(Me)(*o*-C_6H_4OMe) δ 1.81 (d, $J_{PH} = 4$ Hz, Me), 3.85 (s, OMe), 6.80–7.80 (m, aryls); PhP(Me)(CH_2Ph) δ 1.20 (d, $J_{PH} = 4$ Hz,

---

(12) (a) Chatt, J.; Leigh, G. J. *Angew. Chem., Int. Ed. Engl.* **1978**, *17*, 400. (b) Mc Ewen, W. E.; Lau, K. W. *J. Org. Chem.* **1982**, *47*, 3595.

(13) Verkade, J. G. *Coord. Chem. Rev.* **1972–1973**, *9*, 1.

(14) Pregosin, P. S.; Kunz, R. W. *NMR Basic Prin. Prog.* **1979**, *16*, 28.

(15) (a) Bertrand, R. D.; Ogilvie, F. B.; Verkade, J. G. *J. Am. Chem. Soc.* **1970**, *92*, 1908. (b) Ogilvie, F. B.; Jenkins, J. M.; Verkade, J. G. *J. Am. Chem. Soc.* **1970**, *92*, 1916.

(16) Mc Farlane, W.; White, R. F. M. "Techniques of High Resolution NMR Spectroscopy"; Butterworths: London, 1972; Chapter 6.

Me), 2.95 (m, CH_2), 6.90–760 (m, aryls); PhP(Me)(α-np) δ 1.63 (d, J_{PH} = 4 Hz, Me), 7.10–8.60 (m, aryls).

B. Phosphinous Esters (R′ = Me, R″ = OMe, OPh; R′ = α-np, R″ = OMe). The reaction mixture obtained from step IA was stirred with pyridine (12 mL) for 12 h at room temperature. Methanol or phenol (0.05 mol) in ether (25 mL) was then added dropwise at −20 °C, followed by triethylamine (7.5 mL), and the reaction mixture was stirred at room temperature for 24 h and then filtered. The precipitate obtained was washed with an ether/pentane mixture (1:3), the solvent removed under vacuum, and the residue dissolved in ether (5 mL) and pentane (45 mL). A few drops of water were added to the stirred solution. The clear solution was separated and the solvent removed under vacuum to give a liquid. Yields: 85 ± 5%.

NMR data (in $CDCl_3$): PhP(Me)(OMe) δ 1.45 (d, J_{PH} = 3 Hz, Me), 3.45 (d, J_{PH} = 7 Hz, OMe), 7.10–7.70 (m, Ph); PhP(Me)(OPh) δ 1.60 (d, J_{PH} = 6 Hz, Me), 6.70–8.00 (m, aryls); PhP(α-np)(OMe) δ 3.65 (d, J_{PH} = 6 Hz, OMe), 7.10–8.60 (m, aryls).

C. Phosphinous Ester and Amide (R′ = O-*t*-Bu, R″ = Me; R′ = NEt_2, R″ = Me). A slight excess (ca. 10%) of commercial methyllithium in ether was added dropwise to each of the stirred reaction mixtures obtained from step IB, at −76 °C (at the end of the addition, violent evolution of methane was observed). Each reaction mixture was then warmed to room temperature and washed with water. The organic layer was separated, solvent was removed, and the remaining liquid was distilled under vacuum. Boiling points: ester, 92 °C (15 mm); amide, 95 °C (20 mm). Yields: 85%.

NMR data (in $CDCl_3$): PhP(Me)(O-*t*-Bu) δ 1.30 (s, O-*t*-Bu), 1.35 (d, J_{PH} = 7 Hz, Me), 7.10–7.70 (m, Ph); PhP(Me)(NEt_2) δ 1.05 (t, J_{HH} = 7 Hz, C–CH_3), 1.45 (d, J_{PH} = 6 Hz, Me), 2.65–3.20 (m, N–CH_2), 7.20–7.60 (m, Ph).

Preparation of Complexes. Preparation of ($FeCH_3(CO)_3(PMe_3)_2$)(BPh_4). A solution of $FeICH_3(CO)_2(PMe_3)_2$[1a] (4.05 g, 0.01 mol) in methanol (100 mL) was mixed with $NaBPh_4$ (4.10 g, 0.012 mol) in methanol (50 mL), and carbon monoxide was bubbled into this mixture at room temperature to yield a white crystalline precipitate. The solid was collected by filtration, washed with methanol, and dried under vacuum; yield 90%. IR and NMR data are given in Table I.

Anal. Calcd for $BC_{34}FeH_{41}O_3P_2$: C, 65.20; H, 6.59; P, 9.89. Found: C, 65.14; H, 6.54; P, 10.18.

Preparation of ($FeCH_3(CO)_3(PMe_3)_2$)(ClO_4). A solution of $AgClO_4$ (2.07 g, 0.01 mol) in THF (50 mL) was added dropwise into $FeICH_3(CO)_2(PMe_3)_2$ (4.05 g, 0.01 mol) dissolved in THF (100 mL) while CO was bubbled in at room temperature. The AgI precipitate was removed by filtration, and the solution was evaporated to dryness. The residue was taken up in methylene chloride (100 mL), and the addition of ether caused precipitation of a white solid, which was collected and dried under vacuum; the yield was quantitative.

IR data (in CH_2Cl_2): ν_{CO} 2084.0 (w, 2 A_1), 2021.0 (vs, A_1 + B_1) cm^{-1}. This iron cation has configuration **2** on the basis of its IR and NMR spectra.

Preparation of $FeXCH_3(CO)_2(PMe_3)_2$. X = Cl. A solution of ($FeCH_3(CO)_3(PMe_3)_2(BPh_4)$) (6.26 g, 0.01 mol) in methylene chloride (50 mL) was reacted with (Ph_4P)Cl (3.73 g, 0.01 mol) in methylene chloride (50 mL) at room temperature and the resulting precipitate of (Ph_4P)(BPh_4) removed by filtration. The solution was evaporated to solids which were dissolved in hexane and refluxed for 1 h to eliminate 1 equiv of CO. The solution was then reduced in volume, and crystallization occurred on cooling. The solid was collected and dried under vacuum; yield 60%.

IR (in hexane): ν_{CO} 2001.5 (s), 1937.5 (s) cm^{-1}. NMR (in $(CD_3)_2CO$): δ 0.34 (t, J_{PH} = 9.5 Hz, $FeCH_3$), 1.52 (apparent triplet, *N* = 8.5 Hz, PMe_3).

X = Br. The procedure was the same as above except that [Ph_3CH_3P]Br was used as the halogenating agent; yield 70%.

IR (in hexane): ν_{CO} 2001.5 (s), 1939.5 (s) cm^{-1}. NMR (in $(CD_3)_2CO$): δ 0.36 (t, J_{PH} = 9.5 Hz, $FeCH_3$), 1.58 (apparent triplet, *N* = 8.5 Hz, PMe_3).

Preparation of (Fe(COMe)(CO)$_2$(PhP(Me)(OMe))(PMe_3)$_2$)$^+$A$^-$ (A = (BPh_4)$^-$, (ClO_4)$^-$). A solution of ($FeCH_3(CO)_3(PMe_3)_2(BPh_4)$) (6.26 g, 0.01 mol) in methylene chloride (50 mL) was cooled to −20 °C and allowed to react with PhP(Me)(OMe) (1.53 g, 0.01 mol) in methylene chloride (25 mL) (method A). After 1 h, addition of cold ether caused precipitation of white crystals, which were collected and washed with cold ether; yield 100%. The IR and NMR spectra (Table I) were obtained below −10 °C to prevent decarbonylation. For A$^-$ = (ClO_4)$^-$ the same procedure was followed.

Preparation of ($FeCH_3(CO)_2L'(PMe_3)_2$)(BPh_4). All these Fe complexes were obtained by using the same procedure (method B). A solution of $FeICH_3(CO)_2(PMe_3)_2$[1a] (4.05 g, 0.01 mol) in methanol (100 mL) was treated with a slight excess (0.012 mol) of L′, and then $NaBPh_4$ (4.10 g, 0.012 mol) in methanol (50 mol) was added. Precipitation was induced by addition of cold ether, as described above. These experiments were carried out at room temperature for L′ = NCMe, py, PMe_3, $P(OMe)_3$, NCCH(Me)Cl, PhP(Me)(NEt_2), PhP(Me)(OMe), PhP(Me)(OPh), and PhP(Me)(O-*t*-Bu) and below −20 °C for L′ = PhP(Me)(*o*-C_6H_4OMe), PhP(Me)(CH_2Ph), and PhP(Me)(Et). Yields were about 80%.

IR and NMR data of Fe complexes are given in Table I.

Analyses of [$FeCH_3(CO)_2L'(PMe_3)_2$][BPh_4] Compounds. L′ = NCMe. Calcd for $BC_{35}FeH_{44}NO_2P_2$: C, 65.75; Fe, 8.73; H, 6.93; P, 9.68. Found: C, 65.58; Fe, 8.18; H, 7.03; P, 8.98.

L′ = py. Calcd for $BC_{38}FeH_{46}NO_2P_2$: C, 67.37; Fe, 8.24; H, 6.84; N, 2.06; P, 9.14. Found: C, 67.17; Fe, 7.86; H, 6.87; N, 1.98; P, 8.99.

L′ = $P(OMe)_3$. Calcd for $BC_{36}FeH_{50}O_5P_3$: C, 59.85; Fe, 7.73; H, 6.97; P, 12.86. Found: C, 59.91; Fe, 7.56; H, 7.15; P, 12.88.

L* = NC-CH(Me)Cl. Calcd for $BC_{36}ClFeH_{45}NO_2P_2$: C, 62.86; Cl, 5.15; Fe, 8.12; H, 6.59; P, 9.00. Found: C, 62.82; Cl, 4.77; Fe, 8.39; H, 6.51; P, 9.23.

L* = PhP(Me)(OMe). Calcd for $BC_{41}FeH_{52}O_3P_3$: C, 65.44; Fe, 7.42; H, 6.96; P, 12.34. Found: C, 64.97; Fe, 7.35; H, 6.80; P, 12.14.

L* = PhP(Me)(O-*t*-Bu). Calcd for $BC_{44}FeH_{58}O_3P_3$: C, 66.51; Fe, 7.02; H, 7.35; P, 11.69. Found: C, 65.78; Fe, 6.81; H, 7.53; P, 11.45.

L* = PhP(Me)(Et). Calcd for $BC_{42}FeH_{54}O_2P_3$: C, 67.21; Fe, 7.44; H, 7.25; P, 12.38. Found: C. 67.08; Fe, 7.25; H, 7.31; P, 12.22.

Preparation of FeI(COMe)(CO)(PMe_3)$_3$. A solution of $FeICH_3(CO)_2(PMe_3)_2$ (4.05 g, 0.01 mol) in hexane (30 mL) was reacted with a slight excess (0.91 g, 0.012 mol) of PMe_3 at 0 °C. A brownish precipiate was formed on cooling to −20 °C that was unstable in solution.

IR (in hexane): ν_{CO} 1939.0 (s) $\nu_{C=O(Me)}$ 1576.0 (m) cm^{-1}.

Preparation of RuI(COMe)(CO)(PMe_3)$_3$. This complex was prepared from $RuICH_3(CO)_2(PMe_3)_2$, by using the same procedure as above.

IR (in hexane): ν_{CO} 1966.0 (s), $\nu_{C=O(Me)}$ 1588.0 (m) cm^{-1}.

These two acetyl Fe and Ru complexes react with $NaBPh_4$ in methanol to yield [$MCH_3(CO)_2(PMe_3)_3$][BPh_4] (method B).

Preparation of (RuR(CO)$_3$(PMe_3)$_2$)(BPh_4). R = CH_3. A solution of $Ru(CO)_3(PMe_3)_2$[17] (0.343 g, 0.001 mol) in methanol (100 mL) was reacted with a methanolic solution (50 mL) of MeI (0.17 g, 0.0012 mol) and $NaBPh_4$ (0.41 g, 0.0012 mol) at room temperature for 1 h, to yield a white crystalline precipitate. The solid was collected by filtration, washed with ether, and dried under vacuum, yield 80%. IR and NMR data are given in table II.

Anal. Calcd for $BC_{34}H_{41}O_3P_2Ru$: C, 60.81; H, 6.15; P, 9.22. Found: C, 60.48; H, 6.02; P, 9.28.

R = CH_2Ph. The procedure was the same as described above, using $PhCH_2Cl$.

IR (in CH_2Cl_2): ν_{CO} 2108.0 (w, A_1), 2043.0 (vs, A_1 + B_1) cm^{-1}. NMR (in $CD_3)_2CO$): δ 2.56 (t, J_{PH} = 5.4 Hz, RuCH_2Ph), 1.73 (apparent triplet, *N* = 8.0 Hz, PMe_3).

Both complexes have configuration **2** on the basis of their IR and NMR spectra.

Preparation of $RuXCH_3(CO)_2(PMe_3)_2$. X = Cl. A solution of [$RuCH_3(CO)_3(PMe_3)_2$][BPh_4] (0.671 g, 0.001 mol) in methylene chloride (50 mL) was reacted with [Ph_4P]Cl (0.373 g, 0.001 mol) in methylene chloride (50 mL) at room temperature. The mixture was worked up in the same manner as described above for $FeClCH_3(CO)_2(PMe_3)_2$; yield 50%.

Anal. Calcd for $C_9ClH_{21}O_2P_2Ru$: C, 30.05; Cl, 9.85; H, 5.88; P, 17.22. Found: C, 31.82; Cl, 9.39; H, 6.00; P, 17.08.

IR (in hexane): ν_{CO} 2021.0 (s), 1951.0 (s) cm^{-1}. NMR (in CD_2Cl_2): δ −0.10 (t, J_{PH} = 8.1 Hz, $RuCH_3$), 1.52 (apparent triplet, *N* = 7.5 Hz, PMe_3).

X = Br. The same procedure was used with [Ph_3MeP]Br as the halogenating agent.

IR (in hexane): ν_{CO} 2023.5 (s), 1954.0 (s) cm^{-1}. NMR (in $(CD_3)_2CO$): δ −0.04 (t, J_{PH} = 8.1 Hz, $RuCH_3$), 1.59 (apparent triplet, *N* = 7.5 Hz, PMe_3).

X = I. The same procedure was used with [Me_4N]I as the halogenating agent. IR and NMR data are given in ref 1c.

Preparation of ($RuCH_3(CO)_2(NCMe)(PMe_3)_2$)($BF_4$). A solution of $RuClCH_3(CO)_2(PMe_3)_2$ (0.359 g, 0.001 mol) in THF (50 mL) was reacted with a THF solution (50 mL) of $AgBF_4$ (0.192 g, 0.001 mol) and MeCN (0.05 g, 0.0012 mol). AgCl was removed by filtration, and the solution was evaporated to a solid, which was dissolved in methylene chloride (100 mL). After filtration, addition of ether gave a white solid, which was collected and dried under vacuum; yield 90%. IR and NMR data are given in Table II.

Preparation of ($RuCH_3(CO)_2L^*(PMe_3)_2$)(BF_4). All these Ru complexes were obtained by using the same procedure (method C) except for

---

(17) Collman, J. P.; Roper, W. R. *J. Am. Chem. Soc.* **1965**, *87*, 4008.

L* = PhP(Me)(α-np). A solution of $[RuCH_3(CO)_2(NCMe)(PMe_3)_2][BF_4]$ (0.584 g, 0.001 mol) in methylene chloride (100 mL) was reacted with 1 equiv of the corresponding phosphine L* at room temperature for $^1/_2$ h. The complex was precipitated by addition of pentane. The white solid was collected, washed, and dried under vacuum; yields were quantitative. IR and NMR data are given in Table II.

Anal. Calcd for $BC_{20}F_4H_{38}O_3P_3Ru$ (L* = PhP(Me)(O-*t*-Bu)): C, 39.55; H, 6.31; P, 15.30. Found: C, 39.42; H, 6.27; P, 14.91.

Preparation of $(RuCH_3(CO)_2(PhP(Me)(\alpha\text{-np}))(PMe_3)_2)(BPh_3)$. This complex was obtained from $RuICH_3(CO)_2(PMe_3)_2$ by using the procedure described above for $[FeCH_3(CO)_2L^*(PMe_3)_2][BPh_4]$, at −20 °C (method B).

Preparation of $(RuCH_2Ph(CO)_2(PhP(Me)(O\text{-}t\text{-}Bu))(PMe_3)_2)(BF_4)$. A solution of $[RuCH_2Ph(CO)_3(PMe_3)_2]_1[BPh_4]$ (0.747 g, 0.001 mol) in methylene chloride (100 mL) was reacted with 1 equiv of PhP(Me)(O-*t*-Bu) 0.195 g, 0.001 mol) in methylene chloride (50 mL) for 1 h at 20 °C to eliminate 1 equiv of CO (method A). The complex was precipitated by addition of pentane. The white solid was collected, washed, and dried under vacuum.

IR and NMR data are given in Tables II and IV.

Acknowledgment. The authors are indebted to Dr. C. Brevard (Bruker) for the computer simulation of X_9ABY_9 spin systems and for running the ^{13}C spectrum at 62.8 MHz. We also thank Dr. C. Charrier (Laboratoire SNPE, CNRS, Thiais, France) for measuring the ^{31}P spectra, M. J. Pouet for recording ^1H spectra, and Prof. J. F. Harrod and Prof. M. J. Mc Glinchey for helpful discussions.

Registry No. **1**·BPh_4 (M = Fe, L* = NCMe, R = Me), 89616-74-0; **1**·BPh_4 (M = Fe, L* = py, R = Me), 94249-34-0; **1**·BPh_4 (M = Fe, L* = PMe_3, R = Me), 89616-71-7; **1**·BPh_4 (M = Fe, L* = $P(OMe)_3$, R = Me), 89557-49-3; **1**·BPh_4 (M = Fe, L* = NCCH(Me)Cl, R = Me), 94249-36-2; **1**·BPh_4 (M = Fe, L* = PhP(*o*-C_6H_4OMe)(Me), R = Me), 94278-56-5; **1**·BPh_4 (M = Fe, L* = PhP(CH_2Ph)(Me), R = Me), 94249-54-4; **1**·BPh_4 (Me = Fe, L* = PhP(Me)(Et), R = Me), 94249-42-0; **1**·BPh_4 (M = Fe, L* = PhP(Me)(NEt_2), R = Me), 94249-56-6; **1**·BPh_4 (M = Fe, L* = PhP(Me)(OMe), R = Me), 94249-38-4; **1**·BPh_4 (M = Fe, L* = PhP(Me)(OPh), R = Me), 94249-58-8; **1**·BPh_4 (M = Fe, L* = PhP(Me)(O-*t*-Bu), R = Me), 94249-40-8; **1**·BPh_4 (M = Fe, L* = PhP(Me)(OMe), R = COMe), 94249-32-8; **1**·ClO_4 (M = Fe, L* = PhP(Me)(OMe), R = COMe), 94278-52-1; **1**·BF_4 (M = Ru, L* = NCMe, R = Me), 94249-50-0; **1**·BF_4 (M = Ru, L* = PPh_3, R = Me), 94278-58-7; **1**·BF_4 (M = Ru, L* = PMe_3, R = Me), 94249-60-2; **1**·BF_4 (M = Ru, L* = PhP(OMe)(α-np), R = Me), 94249-62-4; **1**·BF_4 (M = Ru, L* = PhP(Me)(α-np), R = Me), 94249-52-2; **1**·BF_4 (M = Ru, L* = PhP(*o*-C_6H_4OMe)(Me), R = Me), 94249-64-6; **1**·BF_4 (M = Ru, L* = PhP(Me)(CH_2Ph), R = Me), 94249-66-8; **1**·BF_4 (M = Ru, L* = PhP(Me)(O-*t*-Bu), R = Me), 94249-68-0; **1**·BPh_4 (M = Ru, L* = PhP(Me)(α-np), R = Me), 94278-59-8; **1**·BF_4 (M = Ru, L* = PhP(Me)(O-*t*-Bu), R = CHPh), 94278-54-3; **2**·BPh_4 (M = Fe, R = Me), 82660-92-2; **2**·ClO_4 (M = Fe, R = Me), 94294-06-1; **2**·BPh_4 (M = Ru, R = Me), 94249-45-3; **2**·BPh_4 (M = Ru, R = CH_2Ph), 94249-47-5; **4** (M = Fe, X = Cl), 78306-62-4; **4** (M = Fe, X = Br), 78306-64-6; **4** (M = Fe, X = I), 33542-07-3; **4** (M = Ru, X = Cl), 94345-81-0; **4** (M = Ru, X = Br), 94249-48-6; **4** (M = Ru, X = I), 88003-88-7; **5** (M = Fe, L* = PMe_3, X = I), 94345-80-9; **5** (M = Ru, L* = PMe_3, X = I), 94249-43-1; $Ru(CO)_3(PMe_3)_2$, 75687-45-5; Me_2Cd, 506-82-1; (α-np)$_2$Cd, 66338-72-5; PhP(Me)Cl, 15849-86-2; (α-np)P(Me)Cl, 94235-64-0; PhP(O-*t*-Bu)Cl, 94235-65-1; PhP(NEt_2)Cl, 4073-31-8; PhP(Me)(*o*-C_6H_4OMe), 1485-88-7; PhP(Me)(CH_2Ph), 23275-37-8; PhP(Me)(α-np), 38851-76-2; PhP(Me)(OMe), 94235-66-2; PhP(OMe)Ph, 4020-99-9; PhP(α-np)OMe, 94278-51-0; PhP(Me)(O-*t*-Bu), 94249-30-6; PhP(Me)(NEt_2), 708-90-7; PhP(Me)(Et), 15849-84-0; (Ph_4P)Cl, 2001-45-8; (Ph_3MeP)Br, 1779-49-3; NCCH(Me)Cl, 1617-17-0; dichlorophenylphosphine, 644-97-3.

Contribution from the Department of Radiology, Division of Nuclear Medicine,
State University of New York Downstate Medical Center, Brooklyn, New York 11203

Formation and Stabilization of Anionic Metal Complexes in Concentrated Aqueous Quaternary Ammonium Salt Solutions

F. L. ARONSON, L. L.-Y. HWANG, N. RONCA, N. A. SOLOMON, and J. STEIGMAN*

Received November 17, 1983

Anionic complexes of transition metals were stabilized in aqueous solutions containing high concentrations of various short-chain quaternary ammonium salts. Compounds with longer paraffin chains were effective in much less concentrated solution. Complex ions were detected spectrophotometrically. $FeCl_4^-$, which is usually formed in concentrated HCl, was the predominant Fe(III) complex in 30 *m* choline chloride containing only 0.12 M HCl. A yellow transitory Tc(VII) chloro-addition intermediate, formed in the reduction of TcO_4^- by concentrated HCl, was stabilized when the solution also contained 25 *m* choline chloride. Its spectrum, as well as the isolation of an already known Tc(VII) bipyridyl complex, is reported. Concentrated organic electrolytes also stabilized Tc(V) oxide halides against disproportionation and Tc(IV) hexahalides against hydrolysis. Halochromates of Cr(VI) were formed and stabilized in dilute acid containing quaternary ammonium salts. Their UV spectra showed the well-resolved vibronic fine structure associated with the symmetric chromium-to-oxygen charge-transfer band. It is known that these progressions are resolved in aprotic solvents, but not in aqueous acidic solution alone, and that the loss of fine structure in aqueous media is due to hydrogen bonding. The stabilization of anionic metal complexes and the resolution of vibronic structure in halochromates are probably consequences of water-structure-enforced ion pairing. The present work strongly suggests that the water molecules in immediate contact with the complex anions are more strongly hydrogen bonded to each other than to the complex.

Introduction

Quaternary ammonium salts of large anions, tetraalkylammonium perchlorates and perrhenates, for example, are considerably less soluble in water than in organic solvents. This illustrates a well-known general phenomenon—that compounds composed of two large ions, although insoluble in water, are often soluble in a variety of organic solvents—and has led to the widespread practice in inorganic chemistry of precipitating such compounds from water and then dissolving them in organic solvents for detailed physicochemical studies. It is particularly useful for the preparation and study of easily hydrolyzable anionic metal complexes.

On the other hand, quaternary ammonium salts in concentrated aqueous solution are salting-in agents.[1] Tetra-*n*-butylammonium perchlorate, for example, is strongly salted into water by concentrated tetra-*n*-butylammonium bromide in spite of the common ion effect.[2] This suggests that quaternary ammonium salts might salt in anionic metal complexes.

There is also reason to believe that concentrated aqueous solutions of quaternary ammonium salts would stabilize as well as solubilize reactive metal complexes. This is suggested by results of extraction studies with strongly basic anion-exchange resins. Such resins, which can be viewed as three-dimensional insoluble

---

(1) (a) Long, F. A.; Bergen, R. L., Jr. *J. Phys. Chem.* **1954**, *58*, 166–168. (b) Gordon, J. E. "The Organic Chemistry of Electrolyte Solutions"; Wiley: New York, 1975; pp 91–92.

(2) Steigman, J.; Dobrow, J. *J. Phys. Chem.* **1968**, *72*, 3424–3436.

0020-1669/85/1324-0541$01.50/0